New Design Considerations for the Calibration of Rubber-Like Materials

Y. Lev & K.Y. Volokh
Faculty of Civil and Environmental Engineering
Technion Institute of Technology, Haifa, Israel

A. Faye
Department of Mechanical Engineering
Indian Institute of Technology, Bhilai, India

Abstract

Rubber-like materials have unique characteristics that make them industrially very attractive. These materials can reach up to stretches of about 6-7 while staying hyper-elastic. Only a few studies that deal with these high level up to failure stretches are available. In addition, information regarding the temperature effect on fracture is absent in the literature.
This work summarizes some recent aspects regarding the calibration of rubber-like materials reaching ultimate deformation (strength) under high operating temperatures.
Our approach to modelling rubber fracture is based on the elasticity with energy limiters theory. Constitutive relations have been developed to generalize this description in order to include the thermo-elastic behavior. A relation for the temperature dependent energy limiters, and a new form for the thermal energy contribution are offered.
The presented theory is used for calibration of rubber-like materials using LS-DYNA®. Our work also includes the design and set-up of a homemade test chamber for the uniaxial and bulge test (inflation of balloon test) cases. These tests are subjected to temperatures in the range of 25℃ to 90℃. The equi-biaxial conditions are extracted indirectly from the bulge test data by performing iterative finite element simulations that are done up to a sufficient fit to the bulge experiment results.
The importance of a simultaneous calibration using both uniaxial and biaxial load cases together is highlighted. Material parameters found are significantly better than the parameters extracted by rubber manufacturers and labs that usually use uniaxial tests in room temperature only.
The methodology used allows the correct modeling of ultimate properties as a function of high common operating temperatures for rubber-like materials.
The findings can serve as new design considerations for engineers using these materials.

Introduction

Thanks to the stable production and process control available today, rubber-like materials are increasingly used and produced in large quantities with consistent properties. The correct description of rubber-like materials for modelling is crucial, but today's standards don't define which exact experiments are needed in order to determine the mechanical properties of rubber-like materials. This is especially true for the case of ultimate deformation (strength), and the effect of temperature on ultimate strength and elongation.
In recent years, Volokh has proposed a new approach to modelling fracture based on elasticity with energy limiters (see [1-4] for detailed description). Our work is based on this theory.
The first part of this work demonstrates the energy limiter theory and its numerical implementation. The user-defined material subroutine of LS-DYNA [5] is used. Simulations of cracks running in a thin pre-stretched rubber sheet are presented and compared to the published DPMS experiments [7-8].

The next part of this work displays the generalized thermo-elastic energy limiter theory developed. A new suggested form of the thermal energy in the material model, and a new relation for the temperature related ultimate values are offered.
The calibration of the theory needs to rely on tests. The high stretches of rubber-like materials can reach up to ~ 7-8 before failure, which makes it difficult to test them under a temperature controlled environment. Most environmental chambers integrated with commercially available load frames are not suitable to accommodate such large stretches. To overcome this issue, we have prepared self-made uniaxial and equi-biaxial test setups with a temperature controlled environment, that can accommodate sufficiently large stretches. We present tests done on the widely industrial used material; Nitrile Butadiene Rubber (NBR).
For the equi-biaxial configuration we adopt the well-known bulge test (inflation balloon or balloon test) [9-11]. The tests are done up to failure at four different controlled temperature steps; 25 ℃, 50℃, 75℃, 90℃. Pressure inside the inflating balloon and the height at the balloon pole are measured for each temperature. Switching to an equi-biaxial stress-stretch representation is done through an iterative FE model simulating the bulge tests. Uniaxial tests are done to the same material and temperature steps up to failure. With regard to both test cases - equi-biaxial and uniaxial - a new set of material parameters are extracted based on a simultaneous fit. Critical biaxial envelopes for each temperature step are built according to the ultimate stretches found. A new relation for the attached dependence of the energy limiter on the temperature is determined, which allows a new design consideration of the temperature related ultimate values.

Energy Limiter Theory and Numerical Implementation

The Cauchy stresses for incompressible materials is determined by

$$\boldsymbol{\sigma} = \left(\det \mathbf{F}\right)^{-1} \frac{\partial W}{\partial \mathbf{F}} \mathbf{F}^T - \kappa \mathbf{1} \tag{1}$$

where $\mathbf{F}$ is the deformation gradient tensor and $\mathbf{1}$ is the identity tensor. The arbitrary scalar parameter known as the 'indeterminate Lagrange multiplier' is denoted as κ .
W is a traditional strain energy function without ultimate values. The basic idea of the fracture theory adopted here is to introduce an energy limiter in the expression for the strain energy function, which indicates the maximum amount of energy that can be stored and dissipated by the material volume during rupture.
The strain energy function including the failure formulation, is given by

$$\psi = \frac{\phi}{m}\left[\Gamma\left(\frac{1}{m},0\right) - \Gamma\left(\frac{1}{m},\frac{W^m}{\phi^m}\right)\right] \tag{2}$$

where $\Gamma\left(s,x\right) = \int_x^s t^{s-1}e^{-t}dt$ is the upper incomplete gamma function. ϕ is the energy limiter that needs to be calibrated from tests. m is a dimensionless parameter controlling the sharpness of transition to the material failure on the stress-strain curve. By increasing/decreasing m it is possible to simulate more or less steep ruptures of the internal bonds. Assuming a brittle failure behavior we use values of at least $m = 10$. Further increase of this parameter does not affect results and the differences are negligible.
We now use the modified strain energy function from eq.2 to determine the Cauchy stresses:

$$\boldsymbol{\sigma} = \left(\det \mathbf{F}\right)^{-1} \frac{\partial \psi}{\partial \mathbf{F}} \mathbf{F}^T - \kappa \mathbf{1} \tag{3}$$

Assuming incompressible materials we have $\det \boldsymbol{F} = 1$ or in principal stretch directions he T . $\lambda_1\lambda_2\lambda_3 = 1$ following uniaxial and equi-biaxial formulations can be determined as follows.
For the **uniaxial case**, the stretch conditions are $\lambda_1 = \lambda, \quad \lambda_2 = \lambda_3 = 1/\sqrt{\lambda}$, and the principal Cauchy stresses are $\sigma_1 = \sigma, \quad \sigma_2 = \sigma_3 = 0$. Placing these conditions and eq.2 in eq.3 we derive the uniaxial Cauchy stress

$$\sigma = 2\exp\left(-\frac{W^m}{\phi^m}\right)\left(\lambda^2 - \frac{1}{\lambda}\right)\left[\frac{\partial W}{\partial I_1} + \frac{\partial W}{\partial I_2}\frac{1}{\lambda}\right] \tag{4}$$

where I_1 and I_2 are the first and second invariants respectively.

For the **equi-biaxial case**, the stretch conditions are $\lambda_1 = \lambda_2 = \lambda, \quad \lambda_3 = 1/\lambda^2$, and the principal Cauchy stresses are $\sigma_1 = \sigma_2 = \sigma, \quad \sigma_3 = 0$. Placing these conditions and eq.2 in eq.3 we derive the equi-biaxial Cauchy stress

$$\sigma = 2\exp\left(-\frac{W^m}{\phi^m}\right)\left(\lambda^2 - \frac{1}{\lambda^4}\right)\left[\frac{\partial W}{\partial I_1} + \frac{\partial W}{\partial I_2}\lambda^2\right] \tag{5}$$

Next, we take as an example the Yeoh hyper-elastic model [12]

$$W = \left(\sum_{k=1}^{3} c_k \left(I_1 - 3\right)^k\right) \tag{6}$$

with material constants from [10] $c_1 = 0.298\,MPa$, $c_2 = 0.014\,MPa$, $c_3 = 0.00016\,MPa$.

The energy limiter value $\phi = 82\,MPa$ is found from the ultimate uniaxial stretch condition of $\lambda_{cr} = 7.12$ [10].

Figure 1 presents the Cauchy stress vs. stretch for uniaxial (eq.4) and equi-biaxial (eq.5) cases, with and without the energy limiter.

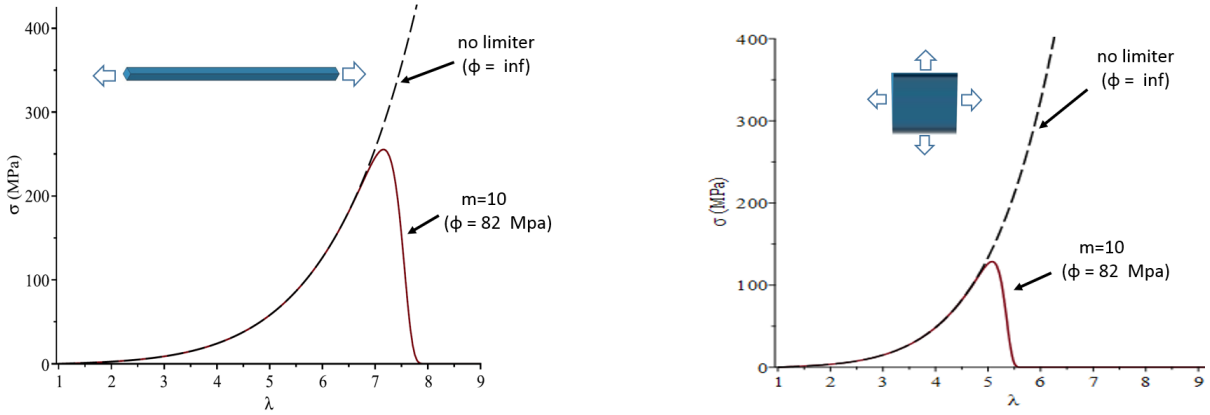

Figure 1: Cauchy stress vs. stretch. Left - uniaxial tension. Right – equi-biaxial tension. Dashed line – with no failure description. Red continues line – with energy limiter

As can be observed, the limiter induces stress bounds in the constitutive equations automatically. Hamdi et al. [10] have conducted different biaxial tests up to rupture with the natural rubber material. An ultimate biaxial chart using the Yeoh model (Eq.6) is presented in Figure 2. The triangles represent ultimate biaxial results. The stars are analytical results derived by repeating the process mentioned above for different biaxial stretch relations and extracting the critical stretches. The comparison between the tests and the analytical results show a close resemblance. This is despite the fact only one energy limiter value was used which was found from the calibration against the uniaxial test alone.

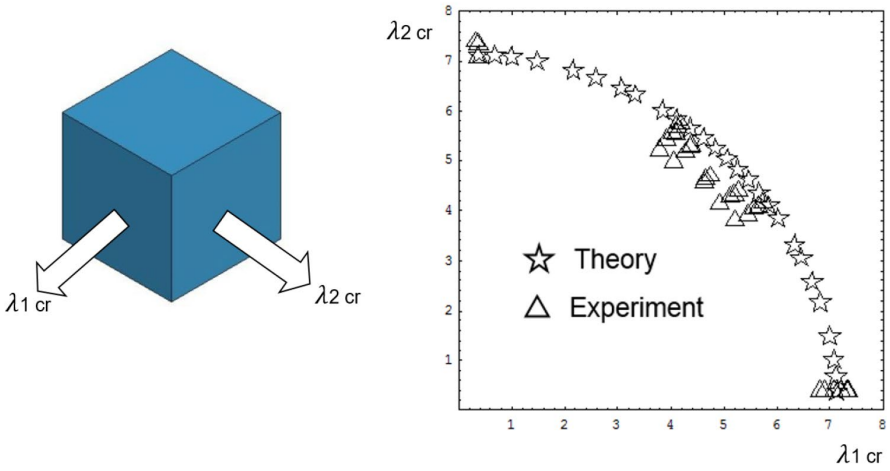

Figure 2: Critical failure stretches in biaxial tension (Volokh, 2010)

Our previous work in [13] has demonstrated a numerical implementation of this theory. The user-defined subroutine was determined using the explicit dynamics version of the LS-DYNA finite element software [5]. User-defined subroutine of the hyper-elastic material model enhanced with the energy limiter are plugged in.
As a numerical example we simulated the DPMS experiments [7-8]. These tests include biaxial pre-stress rubber sheets clamped by a frame. A schematic illustration can be viewed in Figure 3. After initiating a crack (by pricking the stretched rubber sheet at the point marked 'x') a high speed camera measured the speed of the running crack, and the shape of the crack tip.

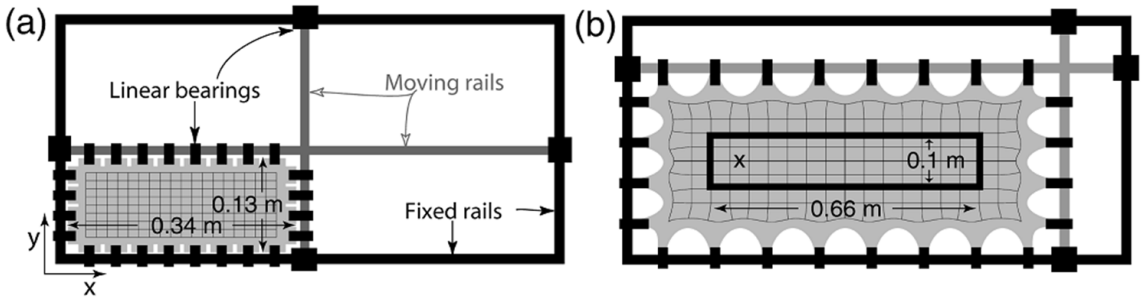

Figure 3: The experimental apparatus for biaxial stretching of rubber sheet [8]

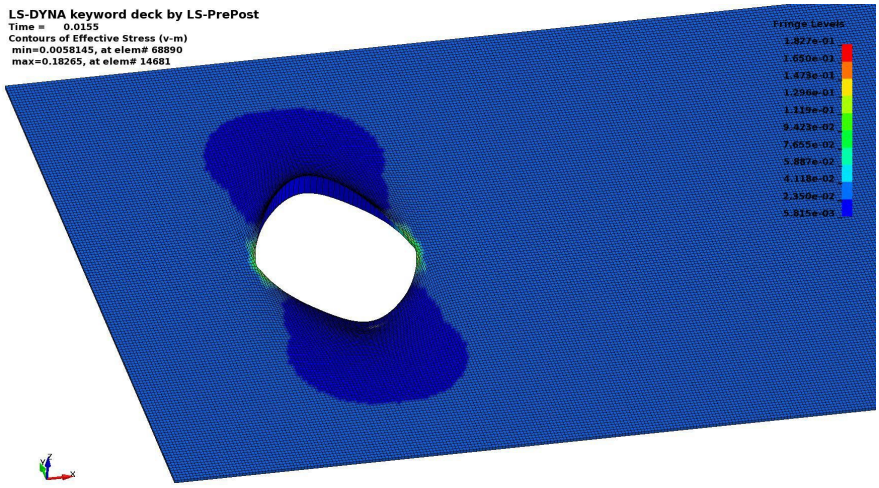

Figure 4: Snap shot of the spontaneously propagating crack, about 15 μ sec after start

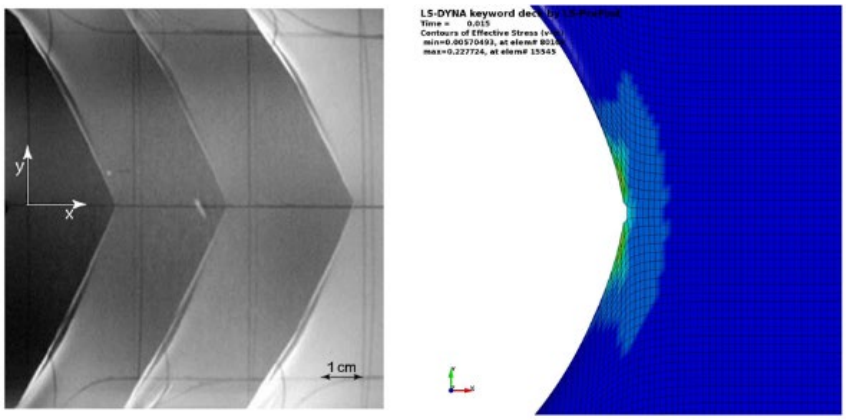

Figure 5: Snapshot of crack tip. Left - Petersan's tests. Right - numerical analysis

The numerical results show a good resemblance to the crack tip shape (Figure 5). A good correlation with the rate of crack tip speed as reported in the DPMS tests is achieved (37 to 60 m/sec).

Generalized Thermo-elastic and Limiter Theory

In this section we generalize the limiter theory to include the temperature dependence. The descriptions described in Eq.2 will now include the temperature dependence for $W(\mathbf{F},T)$ and $\phi(T)$ where T is the current temperature. For the general finite thermo-elasticity theory we refer the reader to [14-15].
The incompressibility condition for which $\det \boldsymbol{F} = \lambda_1\lambda_2\lambda_3 = 1$ typical of most rubber-like materials is modified in the case of the thermo-elastic coupling as follows,

$$\lambda_1\lambda_2\lambda_3 = \exp\left[3\gamma_0\left(T - T_0\right)\right] \tag{7}$$

where γ_0 is a constant of thermal expansion.
The strain energy function for the intact material based on the thermo-elastic generalization becomes

$$W\left(\lambda_1,\lambda_2,\lambda_3,T\right) = \frac{T}{T_0}W_0\left(\lambda_1,\lambda_2,\lambda_3\right) + Q\left(T\right) \tag{8}$$

where W_0, T_0 are the strain energy and temperature at the reference temperature accordingly. $Q(T)$ designates the purely thermal energy which should be concave and positive. Consequently, we have for the heat capacity

$$c = -T\frac{\partial^2 W}{\partial T^2} = -T\frac{\partial^2 Q}{\partial T^2} = c_0\frac{T_0}{T} > 0 \tag{9}$$

We offer a new constitutive relation for $Q(T)$ which is determined by

$$Q\left(T\right) = c_0 T_0 \ln\left[T/T_0\right] \tag{10}$$

For an adiabatic stretching the entropy is constant and we assume a reference state for which the uniaxial stretch $\lambda = 1$ at the reference temperature $T = 293.15K$. Substituting these values and the material constants from Joule's experimental data [16] we find $c_0 = 1.4\left[MPa/K\right]$ (for further details the reader is advised to see [17]).
Assuming the Ogden hyper-elastic model [18] with three sets of material constants:

$$W_0 = \sum_{k=1}^{3}\frac{\mu_k}{\alpha_k}\left(\lambda_1^{\alpha_k} + \lambda_2^{\alpha_k} + \lambda_3^{\alpha_k} - 3\right) \tag{11}$$

where μ_k and α_k are material constants.

The result of placing eq.11 and eq.10 in eq.8 is the generalized strain energy function $W(\mathbf{F},T)$. This can be used in eq.4 or eq.5 for the generalized energy-limiter temperature-dependent uniaxial or equi-biaxial Cauchy stress accordingly.

Thermo-elastic deformation tests and Calibration

The large extension of elastomer's makes it difficult to test with standard equipment including a controlled temperature environment. Thus, the design and development of a test device that have the capacity to carry out tests up to failure at room and higher temperatures are done.
The set-up for conducting uniaxial tests at a constant temperature environment is shown in Figure 6 and the dumbbell shaped specimen used is shown in Figure 7.

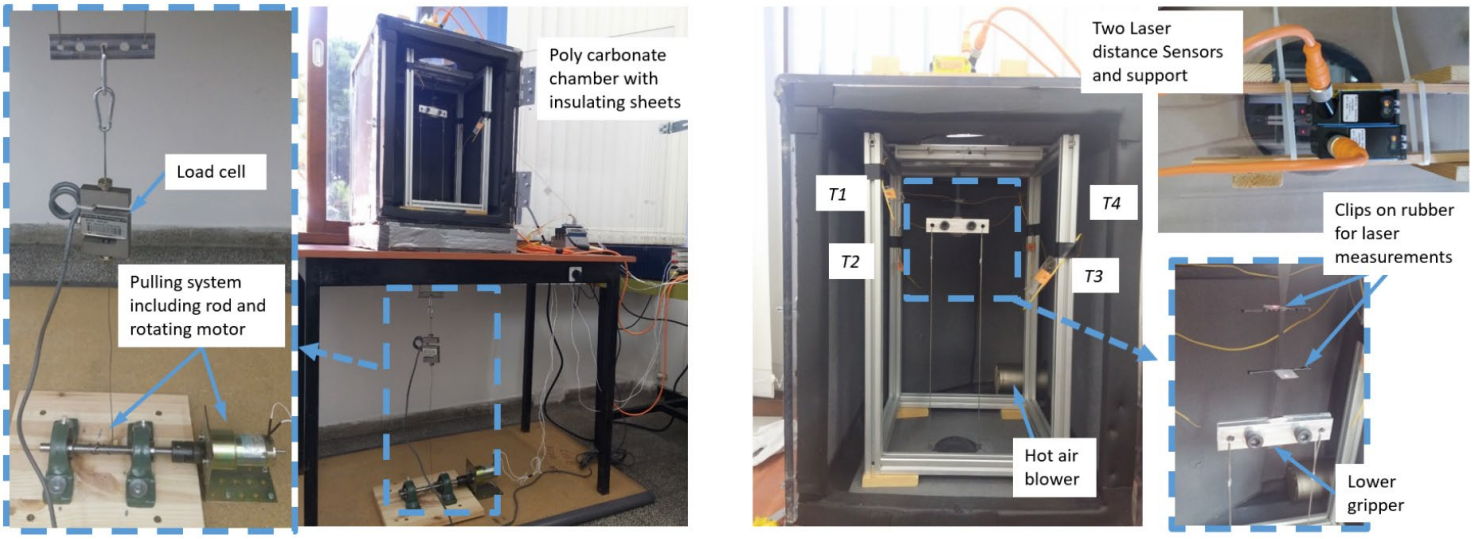

Figure 6: Experimental setup for the uniaxial tension test

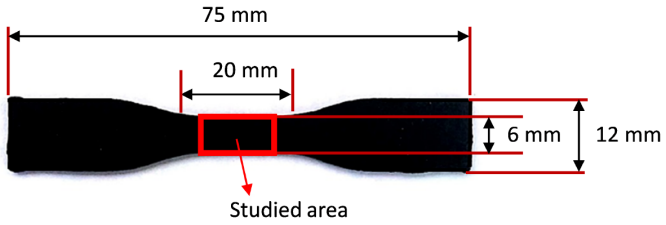

Figure 7: Dimensions of dumbbell rubber specimen for the uniaxial tension test

For the biaxial tests we adopt the well-known bulge test (balloon inflation) [9-11] in order to characterize the equi-biaxial conditions. This procedure involves inflation of a circular rubber sheet, clamped around its edges, by pressurized air under one of its faces (Figure 8). This method is preferable to direct biaxial tension tests since it is not sensitive to imperfections when the specimen is stretched to failure. The pole of the inflated sheet experiences equi-biaxial tension due to axial symmetry of the bulge test configuration.
The schematic view of this set-up is shown in Figure 9.
Both uniaxial and bulge test setups are placed inside a chamber made of Polycarbonate sheets. Walls of the chamber are insulated from inside to prevent heat loss. The temperature inside the chamber is controlled by using a hot-air blower with integrated temperature control. Several thermocouples are placed appropriately to ensure a constant and uniform temperature inside the chamber.

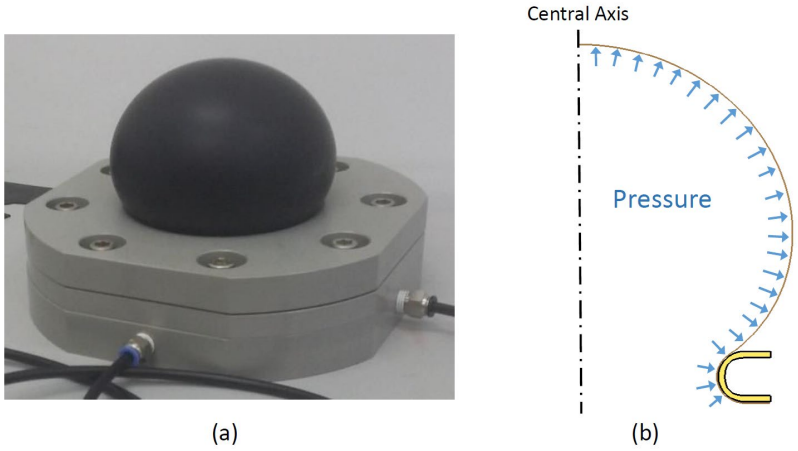

Figure 8: (a) Bulge test device, (b) Schematic view of bulge test.

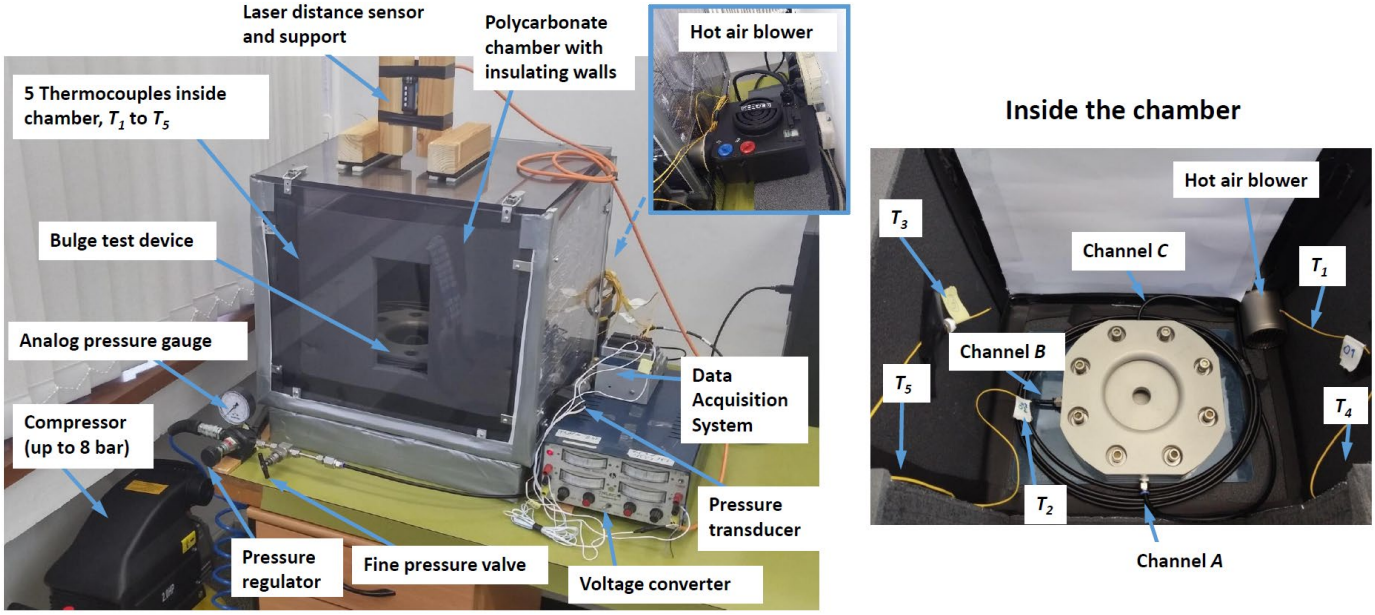

Figure 9: Experimental setup for the bulge test

All the measurements (temperature, pressure, displacement and force) were recorded using a data acquisition card and stored using a LabVIEW program.

The equi-biaxial properties extracted from the bulge tests are achieved indirectly. This is done by using an iterative finite element simulation procedure up to a sufficient pressure versus balloon height fit. Next, the equi-biaxial stress-stretch state found is used together with the uniaxial test results for further calibration of the material model. A simultaneous calibration based on the two sets of data: uniaxial + equi-biaxial data was done according to Ogden et al. [19]. This includes the use of a nonlinear least squares optimization procedure with the help of the Lsqurvefit tool in the optimization Toolbox of MATLAB [20].

It is worth emphasizing the importance of calibrating the material against both uniaxial and equi-biaxial tests through a simultaneous fit. Rubber-like materials are usually subjected to biaxial loading in their real life application. Calibration that is based only on the uniaxial case can lead to an engineering error.

Uniaxial and bulge tests were conducted under a constant temperature environment at 4 different temperatures (25 ℃, 50℃, 75℃, 90℃), for the Nitrile Butadiene Rubber (NBR) material where the average sheet thickness was about 1.2 mm. Summarizing all material parameters found using the simultaneous fit for each temperature step tested are presented in Table 1.

μ_1[MPa]	-3
μ_2[MPa]	-0.002
μ_3[MPa]	0.3563
α_1	-0.0498
α_2	-2.94
α_3	2.5773
Φ[MPa] for 25°C	20
Φ[MPa] for 50°C	42
Φ[MPa] for 70°C	66
Φ[MPa] for 90°C	86

Table 1: NBR material parameters for the three-term generalized thermo-elastic Ogden model with energy limiters (m = 100)

A comparision of the analytical results using these material parameters to the test results at different temperature steps are presented in Figure 10.

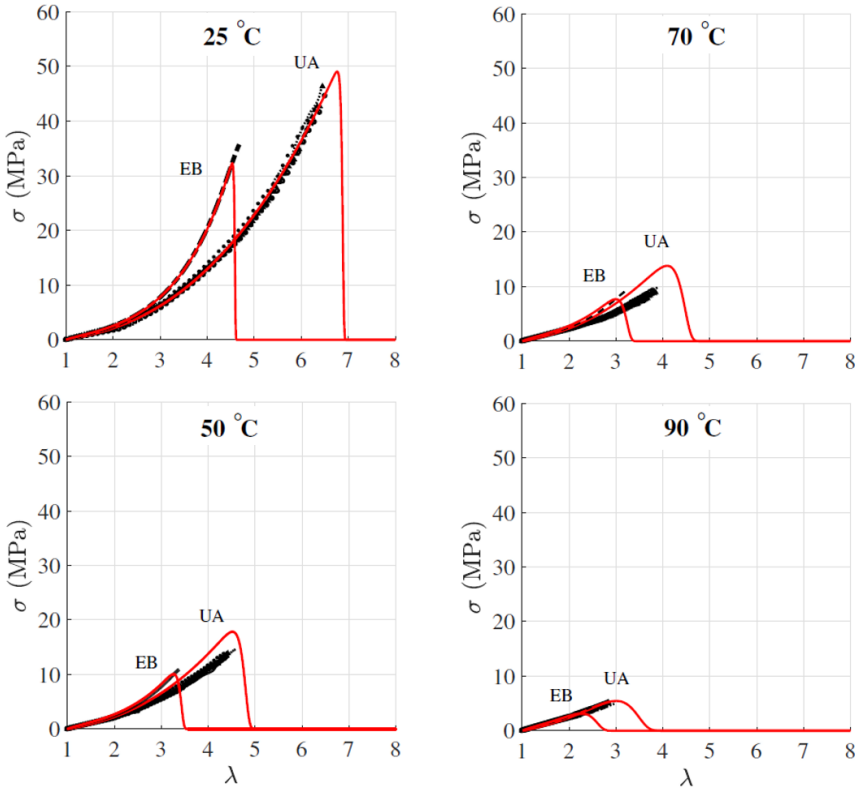

Figure 10: Cauchy stress versus stretch for Nitrile Butadiene Rubber in uniaxial (UA) and equi-biaxial (EB) tension at various temperatures; black for tests and solid red lines for theory.

Figure 11 presents the ultimate biaxial stretch chart for each temperature step. The ultimate stretch values for the uniaxial and equi-biaxial cases were extracted from Figure 10 and placed as stars. Black stars were obtained from tests and red stars from the theory. The red dashed circular line is the best fit achieved from the ultimate results.

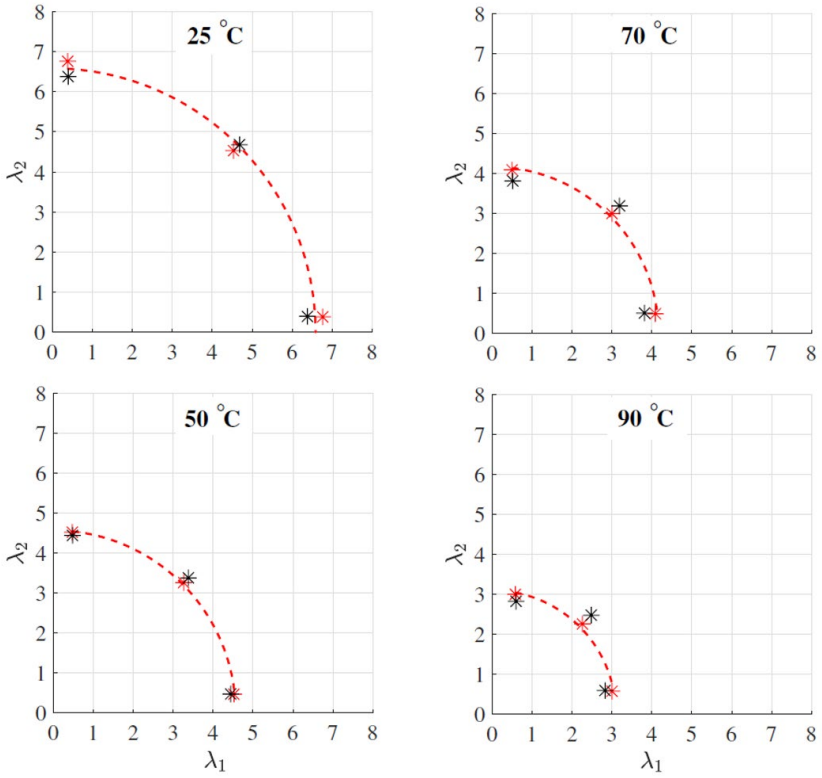

Figure 11: Failure envelope at various temperatures; black for peak test results and red for theory

The results of all biaxial failure envelopes from Figure 11 are given in Figure 12. This offers an effective way for evaluating the material resistance to temperature. It can immediately be observed that the most significant decrease in ultimate biaxial stretches occurs when temperature was raised from 25 ℃ to 50℃. Engineers can also use multiple representations for comparing temperature resistance of different materials.

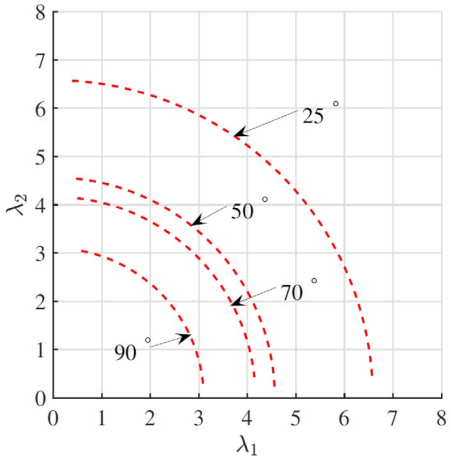

Figure 12: NBR biaxial failure envelopes for each temperature step tested

The desecrate energy limiters values used to build the failure envelopes are placed in Figure 13 together with a linear best fit. This simple linear approximation can be described as

$$\phi(T) = \phi_0 + \beta(T - T_0) \tag{12}$$

where the energy limiter at the reference temperature $\phi_0 = 20\,MPa$ and material constant $\beta = 1.005$.

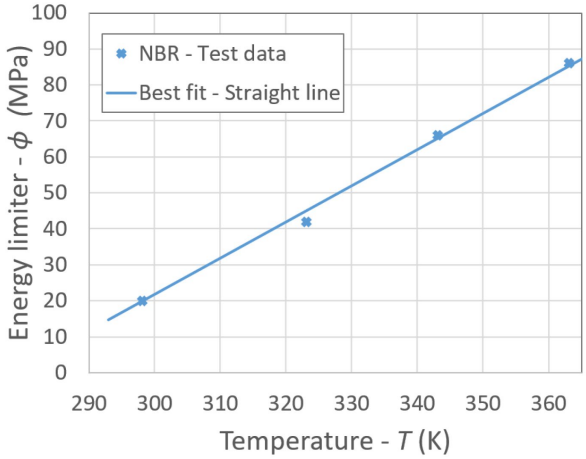

Figure 13: Energy limiter as a function of the temperature.

The suggested relation Eq.12 generalizes the energy limiter theory to include also the temperature effect on ultimate values.

Placing eq.11 and eq.10 in eq.8 is the generalized strain energy function $W(\mathbf{F},T)$ without failure. This relation is used together with Eq.12 to determine the generalized energy limiter theory that couples the temperature effect:

$$\psi(\mathbf{F},T)=\frac{\phi(T)}{m}\left[\Gamma\left(\frac{1}{m},0\right)-\Gamma\left(\frac{1}{m},\frac{W(\mathbf{F},T)^m}{\phi(T)^m}\right)\right] \tag{13}$$

Conclusions

This work has considered experiments and theory concerning the deformation and failure behavior of rubber-like materials. We have started with presenting the energy limiter theory and a demonstration of the FE implementation. Next, we have presented the study of the effect of short-term temperature exposure on the deformation and ultimate properties of rubber-like materials.

Since rubber-like materials can undergo large stretches ($\sim 7-8$ for a uniaxial configuration) before they fail, it is difficult to test under temperature controlled environment. Most environmental chambers integrated with commercially available load frames are not suitable to accommodate such large stretches. To overcome this issue, the design and development of a uniaxial and bulge device that have the capacity to carry out tests up to failure at room and higher temperatures were done.

The material calibration is found using a new suggested form of the thermal energy in the material model, and a new relation for the temperature related ultimate values. This generalizes the theory to include a coupled thermo-elastic up to failure and under the influence of hot service temperatures.

The non-uniqueness of the calibration highlights the importance of performing a simultaneous calibration including both uniaxial and equi-biaxial tests. It was shown that a calibration that is based only on a uni-axial test may show a lack of correlation when the material parameters are used to represent a bi-axial state. Given the fact that rubber-like materials in their industrial application are likely to be subjected to bi-axial loading rather than only uniaxial, there is a great potential for an engineering error. Unfortunately, many manufacturers do only uniaxial calibration probably because it is the easiest to test and calibrate.

From the tests and simultaneous fit, the ultimate stretch values were extracted, and the biaxial ultimate stretch envelope was built. Combining all envelopes found into one graph, the temperature resistance was immediately observed. By repeating this process for different materials, we can compare between the materials resistance to temperature. This can serve as a comparative test for different materials.

Finally, a new simple linear relation between the energy limiter and temperature was suggested for the calibration of a more general thermo-elastic energy limiter theory. This further generalizes the energy limiter theory for use of temperature related ultimate values.

References

[1] Volokh KY (2007) Hyper-elasticity with softening for modeling materials failure. J Mech Phys Solids 55:2237-2264
[2] Volokh KY (2010). On modeling failure of rubberlike materials. Mech Res Commun 37:684-689
[4] Volokh KY (2013) Review of the energy limiters approach to modeling failure of rubber. Rubber Chem Technol 86:470-487
[5] Volokh KY (2014) On irreversibility and dissipation in hyperelasticity with softening. J Appl Mech 81:074501
[6] LS-DYNA Keyword User's Manual, Version 971, Livermore Software Technology Corporation
[7] Deegan, R.D., Petersan, P.J., Marder, M., Swinney, H.L., (2001). Oscillating fracture paths in rubber. Phys. Rev. Lett. 88, 014304
[8] Petersan, P.J., Deegan, R.D., Marder, M., Swinney, H.L., (2004). Cracks in rubber under tension exceeds the shear wave speed. Phys. Rev. Lett. 93, 015504
[9] Charalambides MN, Wanigasooriya L, Williams GJ, Chakrabarti S (2002) Bi-axial deformation of dough using the bubble inflation technique. i. experimental. Rheologica Acta 41(6):532-540
[10] Hamdi A, Abdelaziz MN, Hocine NA, Heuillet P, Benseddiq N (2006) A fracture criterion of rubber-like materials under plane stress conditions. Polymer Testing 25(8):994-1005
[11] Sasso M, Palmieri G, Chiappini G, Amodio D (2008) Characterization of hyper-elastic rubber-like materials by biaxial and uniaxial stretching tests based on optical methods. Polymer Testing 27(8):995-1004
[12] Yeoh O (1990) Characterization of elastic properties of carbon-black-filled rubber vulcanizates. Rubber chemistry and technology 63(5):792{805
[13] Lev Y (2016) Modeling crack propagation in rubber. 14th International LS-DYNA Users Conference
[14] Holzapfel, A.G. , 20 0 0. Nonlinear Solid Mechanics. John Wiley & Sons, Inc. .
[15] Volokh, K.Y. , 2015. Non-linear thermoelasticity with energy limiters. Int. J. Non Linear Mech. 76, 169‑175 .
[16] Joule, J.P. , et al. , 1859. V. on some thermo-dynamic properties of solids. Philos. Trans. R. Soc.Lond. 149, 91‑131.
[17] Lev, Y. , Faye, A. , Volokh, K.Y. , 2018. Experimental study of the effect of temperature on strength and extensibility of rubberlike materials. Exp. Mech. 58 (5), 847‑858 .
[18] Ogden, R.W. , 1997. Non-linear Elastic Deformations. Dover .
[19] Ogden, R.W., Saccomandi G., Sgura I., 2004. Fitting hyper-elastic models to experimental data. Computational Mechanics, 34(6):484–502, 78